Polymacromonomers: Dynamics of Dilute and Nondilute Solutions

Sandra Desvergne, Valérie Héroguez, Yves Gnanou, and Redouane Borsali*

Laboratoire de Chimie des Polymères Organiques, LCPO, CNRS, ENSCPB and Bordeaux-1 University, 16 Avenue Pey Berland 33607 PESSAC Cedex, France

Received June 17, 2004; Revised Manuscript Received January 4, 2005

ABSTRACT: Polymacromonomers (PMs) are a class of branched polymers whose global shape depends strongly on the degree of polymerization of the backbone and the length of the side chain. As opposed to their equivalent linear chains, PMs can indeed adopt spherical, cylindrical, or wormlike shapes. Other parameters such as the rigidity of the side chain, the distance between branches and the interactions (incompatibility) between the backbone and the branches can also contribute to the global morphology of the PMs. In this work we describe the dynamical behavior of several poly(ω-norbornenyl polystyrene) differing by their backbone and their side chain lengths, in dilute and nondilute ranges of concentration, using dynamic light scattering and viscosity experiments. The results obtained, using both techniques, suggest dense and nonentangled particles as revealed by the low viscosity values and the scaling laws observed for the variation of the diffusion coefficient as a function of the molar mass and the concentration c. The transition from dilute to nondilute regime is characterized by an abrupt increase of the diffusion coefficient with the concentration, as opposed to the case of linear and flexible polymer coils. Above this concentration, the diffusion coefficient is independent of the molar mass and hardly varies with the concentration. It is identified as reflecting the overall collective motion of the branches. This transition is also observed in the variation of the reduced viscosity η_{sp}/c as a function of c. Similar studies have been carried out on star polymers of roughly same molar mass where no such an abrupt transition was observed.

I. Introduction

Branched macromolecules exhibit specific solution properties due to a higher segment density compared to linear chains of equivalent molar mass and same chemical composition.[1] Such a higher segment density not only affects the intrinsic viscosity but also interactions of excluded volume type. To define unifying principles that would describe the structure as well as the dynamical behavior of branched polymers, studies on the effects of branching on polymer chain dynamics have been carried out in dilute solution using branched architectures such as star-type, comb-shaped polymers, dendrimers, etc. Besides the latter, polymacromonomers[2,3] are another class of branched polymers that have been comparatively less investigated.

Polymacromonomers—referred to as PM from now—result from the homopolymerization of macromonomers, which are polymers ending with terminal reactive unsaturation; upon polymerization, the latter generates the PM backbone to which are attached side chains (branches) on every repeating unit. The PMs investigated in this work have been prepared using ring-opening metathesis polymerization of norbornenyl-terminated macromonomers, a chain addition mechanism which can be carried out under truly "living" conditions.[4,5] The resulting polymers are characterized by a regular branching interval and exhibit expected and narrowly distributed molar masses; they can thus be considered as model compounds. Depending on the degree of polymerization of the backbone ($\overline{DP}_{n\ MC}$), PMs are expected to adopt different shapes. At low $\overline{DP}_{n\ MC}$'s, a spherical distribution of branches prevails over the cylindrical symmetry that characterizes PM of higher $\overline{DP}_{n\ MC}$'s. Besides the size of the backbone, the PM global shape is also known to depend on other parameters such as the length of the side chain ($DP_{n\ SC}$), the distance between branches (type of the macromonomer terminal unsaturation), the rigidity of side chains and the interactions (incompatibility) between the backbone and the branches if both are chemically different.

Scheme 1[a]

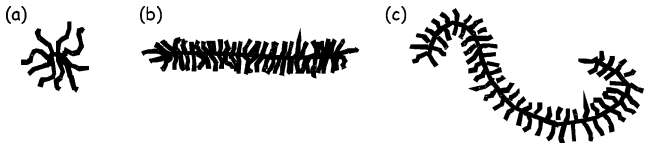

[a] Key: (a) low DP = spherical shape; (b) intermediate DP = anistropic shape (stiff cylinder); (c) high DP = wormlike shape (flexible cylinder).

Experimental,[6−18] computational, and theoretical[19] studies on the behavior of PMs including amphiphilic cylindrical brushes[20,21] have been carried out over the last years. The increase of the persistence length and the change in the PM overall shape from a nearly spherical to a cylindrical distribution of the chain as the size of the side chains increases (Scheme 1) are two observations made from earlier dilute solution work.[22]

In their investigation, Schmidt and co-workers[7] mentioned that PMs of PS (PS branches, PMMA backbone) exhibit in dilute solution an extremely high stiffness (Kuhn's statistical length l_K up to 200 nm) which was found to increase with the molar mass of the side chains but not with the length of the backbone. According to these authors, rodlike macromolecules may well be prepared from "commodity" monomers, and one can expect these structures to exhibit a lyotropic behavior.

PMs have also been analyzed by scanning force microscopy.[13−15] These studies show that the formation of a mesomorphic phase also depends on the same

* Corresponding author. E-mail: borsali@enscpb.fr.

10.1021/ma0487958 CCC: $30.25
Published on Web 02/10/2005

Scheme 2: Polymacromonomer from ω-Norbornenyl Polystyrene Macromonomers

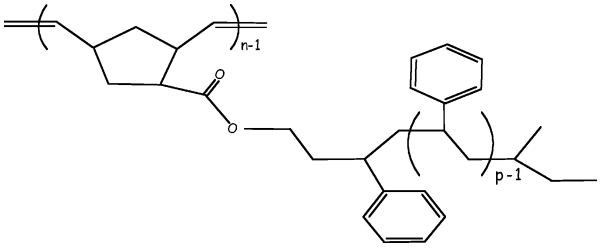

parameters that are the lengths of the side chains and of the backbone. Repulsive interactions between the side chains enhance the main chain stiffness and hinder the interpenetration of the branches from adjacent molecules. This results in an orientational order of the PMs.

The structure and dynamics of PMs in nondilute solutions and melts have also been investigated and compared to those of multiarm stars.[16] The results obtained reveal an intermediate behavior of the PMs between those characteristics of linear chains and those attributed to high functionality multiarm stars. Their rheological behavior[17,18] indicates that branches of neighboring macromolecules entangle when they are longer than a critical value ($M_{w\ branch} > M_c$) corresponding to the molar mass of the intermolecular chain entanglement of linear PS. For those PMs whose branches are shorter than that critical value, a weak rubbery plateau was observed, provided that their $\overline{DP}_{n\ MC}$ is large enough.

Computational simulations and theoretical calculations are another approach to understand the behavior of PMs. More than a decade ago, Birshtein and coworkers[19] theorized that both the backbone and the side chains should be considerably stretched in PMs because of the excluded volume effect, which should result in a high persistence length. Similar conclusions were also drawn from computer simulations.

The majority of PMs investigated so far have been obtained by homopolymerization of either ω-styryl or ω-methacryloyl macromonomers, which eventually gave rise to dense brush-type polymers with a side chain every two carbons. The PMs investigated in this study are less dense than those described in the literature, each side chain being separated from the next one by six carbons of the main chain (Scheme 2). Whether the ease in the congestion associated with such polynorbornene-based backbone affects the overall behavior of this class of PS-based PMs is one of the questions that will be addressed in this study. In a previous article devoted to these poly(ω-norbornenyl polystyrene) PMs,[20] the evolution of the intrinsic viscosity has been analyzed as a function of $\overline{DP}_{n\ MC}$. Two behaviors typical of spherical and rod-/wormlike objects were observed for low and high $\overline{DP}_{n\ MC}$'s respectively. Between the two domains a significant decrease in the viscosity could be noticed, due to a shrinkage of the apparent hydrodynamic volume. Similar results were reported by Tsukahara and co-workers[23,24] on their poly(ω-methacryloyl polystyrene) PMs.

In continuation of this first study,[22,25] a more detailed investigation of the behavior exhibited by these poly(ω-norbonenyl polystyrene) PMs (Scheme 2) has been carried out using dynamic light scattering and viscosity measurements (THF medium).[25] More specifically, the effect of both the side chain size and the backbone length has been analyzed. The results are compared to those of PS stars having equivalent molar masses.

II. Experimental Section

II.1. Synthesis and Polymerization of ω-Norbornenyl Polystyrene Macromonomers. Two macromonomers of polystyrene end-fitted with a norbornenyl insaturation were prepared following the procedure described in the literature.[25] Table 1a gathers their characteristics. Starting from each of these macromonomers, several PMs of different $\overline{DP}_{n\ MC}$ were obtained by "living" ring opening metathesis polymerization. Their molecular characteristics are listed in Table 1b and have already been discussed in a previous work.[22,25] In the nomenclature PS*X*-*Y*, *X* and *Y* stand for the macromonomer molar mass and the degree of polymerization of the PM, respectively.

II.2. Sample Preparation. Dilute and semidilute solutions in THF (good solvent) were prepared by dissolving the appropriate amount of PM in the solvent for about 24 h to ensure complete dissolution. All solutions were carefully filtered on 0.22 μm Millipore PTFE filter and the measurements were performed at 25°C. The choice of the PMs to investigate was guided according to the viscosity measurements described in previous studies.[22] The molar masses were chosen in order to study objects exhibiting different global shapes (cf. Table 2). For comparison, a linear polynorbornene has been synthesized ($\overline{DP}_{n\ MC} = 370$) and studied using the same sample preparation and techniques. To be complete in our comparison, four and eight arms star of polystyrene having equivalent molar masses to those of PS2700 PMs have also been investigated by DLS. Their molecular characteristics are listed in Table 1c.

II.3. Dynamic Light Scattering (DLS). The full homodyne autocorrelation functions[26] of the scattered intensity were obtained using the ALV-5000 autocorrelator from ALV, Langen, FRG (at different wavevector $q = (4\pi n/\lambda)\ \sin(\theta/2)$ or scattering angle θ) and Malvern ZetaSizer 3000HSA instrument ($\theta = 90°$). The measured intensity−intensity time correlation function is related to the electric field correlation function by the Siegert relation[27]

$$g^{(2)}(t) = 1 + \beta|g^{(1)}(t)|^2 \tag{1}$$

where β is spatial coherence factor depending upon the geometry of the detection and the ratio of the intensity scattered by polymer to that scattered by the solvent. Generally, $g^{(1)}(t)$ may be expressed by a continuous distribution of decays

$$g^{(1)}(t) = \int A(\Gamma)\ \exp -(\Gamma t)\ \mathrm{d}\Gamma \tag{2}$$

where $g^{(1)}(t)$ is the Laplace transform of the decay rate distribution function $A(\Gamma)$. $A(\Gamma)$ gives the relative intensity of light scattered with decay constant Γ and is a function of the number and size of the scatteres. For a dilute solution of spherical and monodisperse particles undergoing Brownian diffusion $g^{(1)}(t)$ may be represented by

$$g^1(t) \cong \exp(-q^2Dt) \tag{3}$$

where D is the translational diffusion coefficient.

The autocorrelation functions of the scattered intensity were analyzed by means of constrained regularization (CONTIN) method developed by Provencher[28] to obtain the distribution of decay times (or frequencies) and their corresponding amplitude. The diffusion coefficients were calculated from $D = (\Gamma/q^2)_{q\to 0}$ and the converted equivalent hydrodynamic radii R_H were deduced using the Stokes−Einstein relation $D = k_BT/f$. k_BT is the Boltzman energy, $f = 6\pi\eta_S R_h$ (assuming a spherical symmetry) is the friction coefficient and η_0 the solvent viscosity.

In dilute solutions, typical variation of the frequency Γ vs q^2 measured on PS4800-117 using the ALV-5000 goniometer is displayed in Figure 1. Such a variation shows a q^2-behavior (diffusive motion), and the diffusion coefficient is $D = \lim_{q\to 0}$

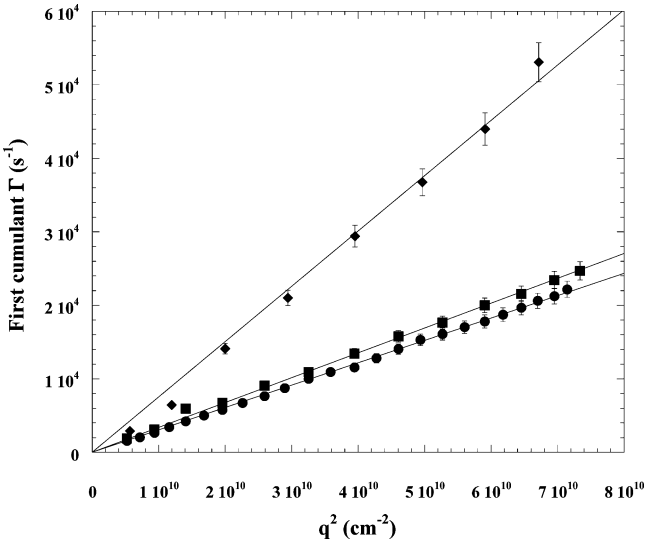

Figure 1. Variation of the frequency Γ vs q^2 for PS4800-117/THF at the concentrations: (●) $c = 0.006$ g·mL^{-1}, (■) $c = 0.015$ g·mL^{-1}, and (◆) $c = 0.040$ g·mL^{-1}.

Γ/q^2. Consequently to the q^2-behavior, all the correlation functions were measured at 90° in scattering angle using Malvern ZetaSizer 3000HSA. The determination of the relaxation time or the frequency from the autocorrelation function $C(q,t)$ was proceeded systematically via the CONTIN method. However, when two relaxation times coexisted, their resolution was not possible by this method when the ratio did not exceed 5. In this case, a two-exponential decay function was used and a good agreement was found.

II.4. Viscosity Measurements. Viscosity measurements were carried out using a Ubbelohde-type flow capillary viscometer. The specific viscosity η_{sp} was measured and the reduced viscosity η_{sp}/c as well as $\ln\eta_r/c$ were plotted as a function of the concentration for the three investigated PMs (branches molar mass = 2700 g mol^{-1}). These measurements were performed to corroborate earlier viscosity measurements and the actual DLS measurements. All solutions were prepared similarly to DLS measurements.

III. Results and Discussion

III.1. Dilute Solutions. DLS measurements have been performed on dilute solutions in a range of concentrations c below 8×10^{-2} g·mL^{-1}. As expected, the autocorrelation functions show one relaxation time and the diffusion coefficient D was found to depend linearly on the concentration (Figure 2a) according to

$$D(c) = D_0(1 + k_D c) \tag{4}$$

with

$$k_D = 2A_2M - v_2 - k_f \tag{5}$$

where k_D is the virial dynamic, A_2 is the second virial coefficient, M is the molar mass, v_2 is the specific volume and k_f is the friction coefficient. From the translational diffusion coefficient extrapolated at zero concentration D_0 (eq 4), the equivalent spherical hydrodynamic radius $R_h{}^0$ was calculated $D = k_BT/f = k_BT/(6\pi\eta_S R_h)$. The results obtained are listed on Table 3. Such calculations of the hydrodynamic radii $R_h{}^0$ are meaningful only for samples PS2700-29 and PS4800-25 (having small $\overline{DP_{n\ MC}}$) exhibiting a spherical shape.

The values found for low molar mass PS2700-29 and PS4800-25, $R_h{}^0_{PS2700-29}$ (6.67 nm) and $R_h{}^0_{PS4800-25}$ (9.62 nm), are very close to the theoretical length of an extended linear PS chain of equivalent molar mass (L_{2700} = 6.45 nm and L_{4800} = 11.63 nm), calculated assuming 0.25 nm for the C−C bond of the vinylic monomer. Knowing the persistence length (l_P = 1.5 nm) of PS this means that short branches in PMs are stretched—if not fully—to a large extent. As a consequence, all further calculations have been performed under the assumption that the diameter of the cross-section remains constant and is equal to twice the hydrodynamic radius of the spherical symmetry. This assumption is valid in the dilute regime.

To calculate the sizes corresponding to a nonspherical symmetry, both prolate/ellipsoid models (relations 6 and 7) and the Yamakawa−Fujii model[29] have been successively used for PM2700-117 and PM2700-345, PS4800-185, and PS4800-290. The prolate ellipsoid model was useful for an evaluation of the approximate length L_{NB} of the object, while the Yamakawa−Fujii model[29] allowed us to determine the Kuhn length l_K ($l_K = 2l_P$). Depending upon the values found for L_{NB} and l_K, these calculations should indicate whether the macromolecules adopt a rodlike shape ($L_{NB} \leq l_P$) or a flexible cylinder conformation ($L_{NB} \gg l_P$).

The prolate ellipsoid model requires two parameters a and b, which are respectively the semimajor and semiminor axes required for the calculation of $D_{0\ calculated}$ that can be compared with experimental values of $D_{0\ experimental}$:

$$D_{0\ calculated} = k_BT/f_0 = k_BT/6\pi\eta_S aG(\rho) \tag{6}$$

and

$$G(\rho) = (1 - \rho^2)^{1/2}/\ln[(1 + (1 - \rho^2)^{1/2})/\rho] \tag{7}$$

where $\rho = b/a$ is the axial ratio. When $a = b = R$, $G(\rho)$ becomes unity; hence, eq 6 reduces to the Stokes−Einstein relation for a hard sphere of radius R.

In our calculations, b was taken equal to $R_h{}^0_{spherical\ shape}$ and a was adjusted so as to match both $D_{0\ calculated}$ and $D_{0\ experimental}$ values. From the knowledge of the length L_{NB} value for the PMs, l_K could be calculated using the Yamakawa−Fujii model. For PS2700-117 and PS4800-185 systems, a rodlike shape is expected. Since l_K is believed not to depend on $\overline{DP_{n\ MC}}$, one can evaluate the length L_{NB} of larger objects, namely PS2700-345 and PS4800-290, expected to exhibit a wormlike conformation. Table 4 summarizes all the results.

Although the values obtained for l_K are not fully reliable due to the method of determination (within an experimental error of 5%), they call for interesting remarks. It appears that $l_{K\ 4800}$ is much larger than $l_{K\ 2700}$, which is consistent with previous studies[6,7] and studies on similar systems[31] using small-angle neutron scattering. This indicates an increase of the persistence length l_P (therefore in the Kuhn statistical length l_K) as the length of the side chains increases. Moreover, the obtained results is consistent with the assumed conformation of the macromolecule:

- L_{NB} PS2700-117 (29 nm) and L_{NB} PS4800-185 (50.3 nm) are smaller than the respective persistence lengths ($l_K/2$ = 34.3 and 57.8 nm, respectively), which is consistent with a rodlike shape,
- L_{NB} PS2700-345 (94.5 nm) and L_{NB} PS4800-290 (82 nm) are longer than the respective persistence lengths ($l_K/2$ = 34.3 and 57.8 nm, respectively), which is indicative of a flexible cylinder conformation

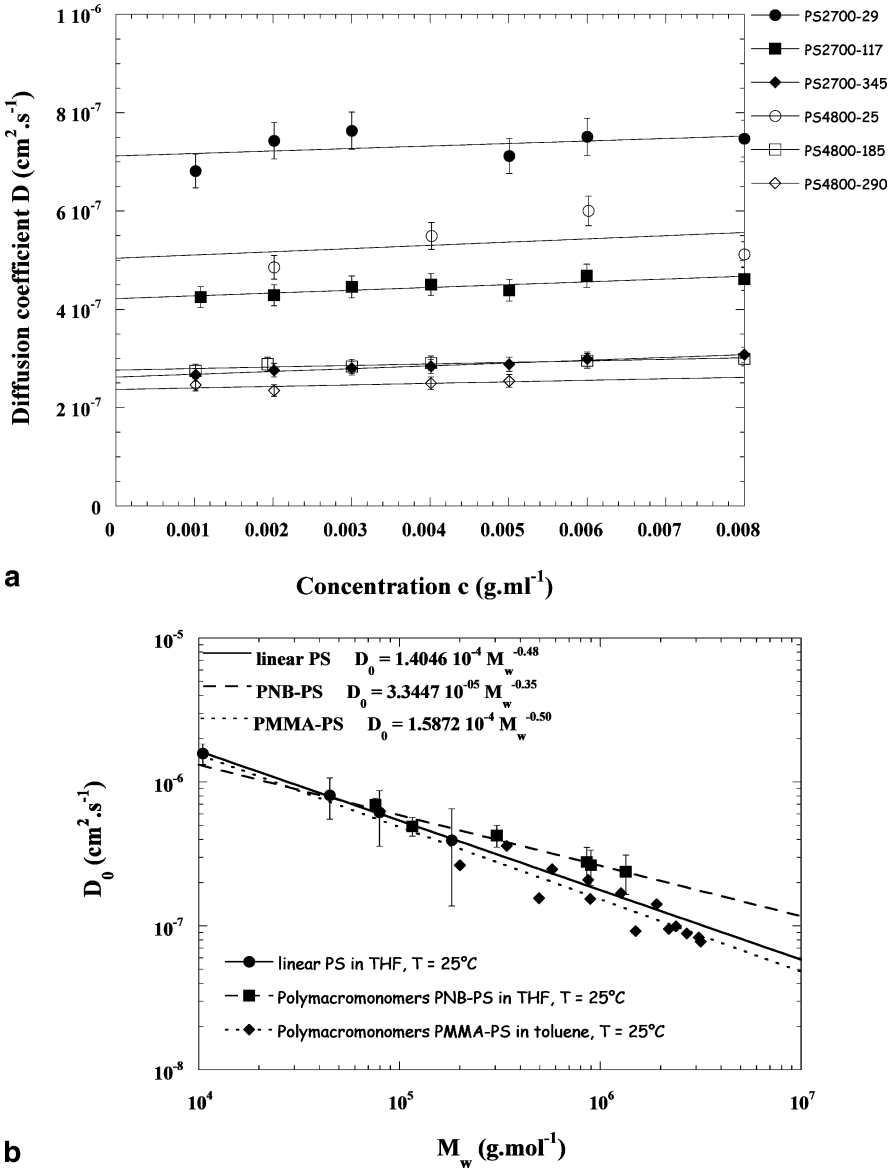

Figure 2. (a) Influence of the backbone length and the branch length PMs NBPS, THF, 25 °C. Dilute domain, $D = f(c)$. (b) PMs NBPS, THF, 25 °C: $D_0 = f(M_w)$ (●) linear PS in THF, $T = 25$ °C,[30] (■) PNB−PS PMs in THF, $T = 25$ °C, and (◆) PMMA−PS PMs in toluene, $T = 25$ °C.[7]

The molar mass dependence of the translational diffusion coefficient D could be deduced from the log D_0 vs log $\overline{M_W}$ plot (Figure 2b): $D_0 \propto \overline{M_W}^{-0.35}$. Although such dependences could be established only within a small range of molar masses, it clearly shows that the solution properties of PMs differ from those exhibited by linear chains $D_0 \propto \overline{M_W}^{-0.48}$ and $D_0 \propto \overline{M_W}^{-0.5}$ shown also in Figure 2b for comparison. The −0.35 slope value determined for PMs indicates that these particles are rather dense (for hard dense spheres, let recall that $M \propto R^3$ and consequently $D_0 \propto \overline{M_W}^{-1/3}$). As the molar mass increases, we expect a deviation from the $-1/3$ scaling law.

III.2. Crossover from Dilute to Nondilute Regimes. In this range of concentration, the autocorrelation functions were described by two relaxation times: fast and slow modes. The slow mode whose amplitude is concentration-dependent was purposely overlooked (see the discussion below). Let recall, however, that the collective dynamics of linear coiled chains in the semidilute regime (above the overlap concentration c^*) exhibits the following scaling laws $D_c \propto c^{0.75}$ and $D_c \propto c$ in good solvent and Θ solvent conditions, respectively. In this range of concentration, D_c is the collective or the cooperative diffusion coefficient that depends only on the concentration and is independent of the molar mass. This dynamical behavior that is clearly observed in numerous binary polymer/solvent systems and characterized by a crossover at the overlap concentration c^* is very well described and documented in the literature and is the consequence of entanglements between linear chains. In this section we will present the dynamical behavior properties of PMs solution and compare them with those of linear coiled polymers having roughly the same molar mass.

The measurements have been performed on all Table 1 listed PMs. In nondiluted solutions, typical correlation functions are illustrated in Figure 3a for this system at $c = 0.030$ g·mL^{-1}for PS2700-based PMs. As opposed to the dilute regime, a single relaxation mode correlation function failed to fit the data in this regime of concentration. Consequently, the correlation functions were

Table 1. Macromonomer (a), PMs (b), and Stars (c) Characteristics

(a) Macromonomer

sample	M_n macromonomers (SEC) (g mol^{-1})	I (given by SEC)	M_n macromonomers (^{1}H NMR) (g mol^{-1})
PS2700	2700	1.04	2900
PS4800	4800	1.03	5300

(b) PMs

sample	M_n macromonomers (SEC) (g mol^{-1})	M_n polymacromonomers LS (10^5 g mol^{-1})	$\overline{DP_{n\ MC}}$ (LS)	global shape
PS2700-29	2700	0.785	29	sphere
PS2700-117	2700	3.159	117	rodlike
PS2700-345	2700	9.315	345	wormlike
PS4800-25	4800	1.200	25	sphere
PS4800-185	4800	8.880	185	rodlike
PS4800-290	4800	13.920	290	wormlike

(c) Stars

sample	M_n stars LS (10^5 g mol^{-1})	no. of branches
StarPS-90	0.893	4
StarPS-500	4.892	8
StarPS-800	7.970	8

adjusted with a 2 exponential-fit and a very good agreement was found (solid lines in Figure 3a). The data were also analyzed using CONTIN and the results show clearly that the dynamics is described by two frequencies as seen in the narrow distribution of relaxation times displayed in Figure 3b.

Similar results were found by other authors[16] in the study of their PMs system (e.g., PS−PMMA) and the relaxation of the slow mode whose amplitude is concentration and angular dependent was regarded as associated with the PM self-diffusion. Similar conclusions can also be drawn for our systems.

Figure 3c captures the dynamical behavior of the PS2700-based PMs (the single mode in dilute regime and the fast cooperative mode in the nondilute regime) and shows the plot of log D vs log c for a large domain of concentrations, ranging from $c = 1 \times 10^{-3}$ g·mL^{-1} to $c = 1 \times 10^{-1}$ g·mL^{-1}.

An abrupt transition is observed in the variation of log D vs c for PM samples and particularly for $\overline{DP_{n\ MC}} = 117$ and 345. These values are 0.012, 0.011, and 0.009 g·mL^{-1}, respectively and are consistent with the molar mass of the PMs. Indeed this transition occurs at concentrations inversely proportional to the molar mass. This transition is certainly related to the concentration at which the PM particles start to "feel" the presence of each other and might be attributed to the crossover from dilute to the semidilute domains. However, and contrary to the smooth classical transition observed for linear polymer coils (crossover at the overlap concentration c^*), an important discontinuity is observed between the two domains of concentration particularly for PS2700-117 and -345. It is the high compactness of the PMs that prevents the branches of neighboring macromolecules from entangling each other and is certainly responsible for this abrupt transition. Conversely, PS2700-29 exhibits a continuous variation of its diffusion coefficient as a function of c and a change of slope can be noticed at 0.012 g·mL^{-1}. The smooth variation of D vs c can be explained on the basis of the low molar mass of the PS2700-29 and more likely to its spherical shape.

On the other hand, the slope of the variation of log D vs log c in the nondilute regime reveals an entirely different scaling law from that of linear chains. $D_c \propto c^{0.2}$, in sharp contrast with linear coiled chains in good solvent ($D_c \propto c^{0.75}$).

The measurements performed on PS4800 -based PM, follow a similar trend. The plot of log D vs log c (Figure 4) for PS4800-185—as for PS2700-117 sample—shows a sharp discontinuity. As the branches are for the PS-4800-based systems longer than for PS-2700 PM, the contact between macromolecules is likely to occur at lower concentrations. As a matter of fact the crossover concentration values determined for PS4800-185 and -290 are lower than those of PS2700-117 and -345 and are respectively equal to 0.008 and 0.005 g·mL^{-1}. In the semidilute region D varies proportionally to $c^{0.266}$ for PS-4800-based PMs.

According to the scaling laws that have been established for both systems (PS2700 and PS4800) in the semidilute domain, samples with a side chain of same size obey a same scaling law whatever their $\overline{DP_{n\ MC}}$, reflecting the importance of the side chain length on the entanglement between neighboring macromolecules. However, those PMs with a low $\overline{DP_{n\ MC}}$ (PS2700-29 and PS4800-25) show faster collective diffusion coefficient values than their homologues of higher $\overline{DP_{n\ MC}}$.

The variation of the cooperative diffusion coefficients measured in all the PM systems as a function of the concentration show a scaling behavior that approaches $D_c \propto c^{1/3}$. If such collective motion is converted into a correlation length $\xi \propto c^{-1/3}$, it becomes clear that these particles are dense and not entangled and present a uniform distribution. These features are completely different from those known for the coiled polymeric systems. Indeed, for flexible coiled and entangled polymer chains, ξ scales with the concentration as $c^{-3/4}$, where ξ represents the mesh size of the formed pseudo-network.

The observed transition from dilute to the nondilute regime is characterized by an abrupt increase of the diffusion coefficient with the concentration that is not observed in the case of linear and flexible polymer coils. Above this concentration, the diffusion coefficient is found independent of the molar mass and weakly varies with the concentration. One may ascribed this peculiar transition to a dynamics that reflects the overall col-

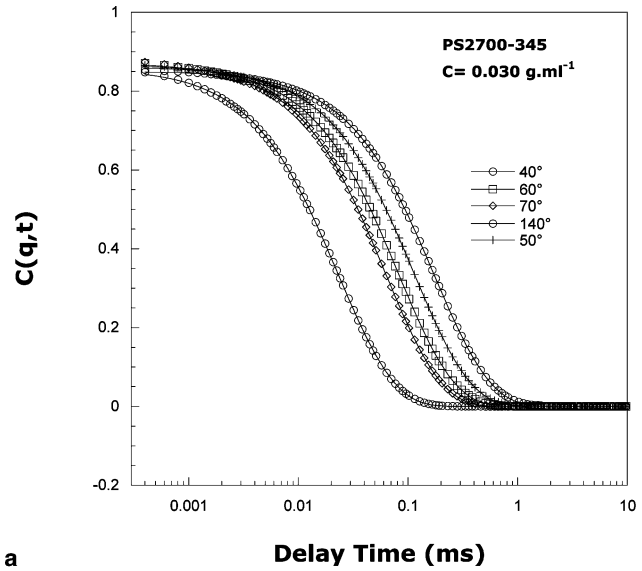

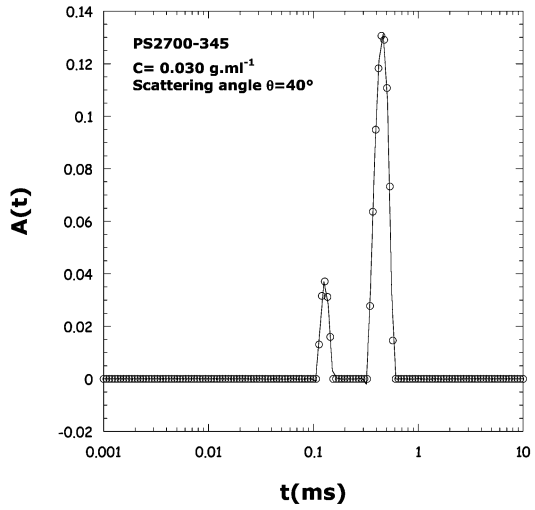

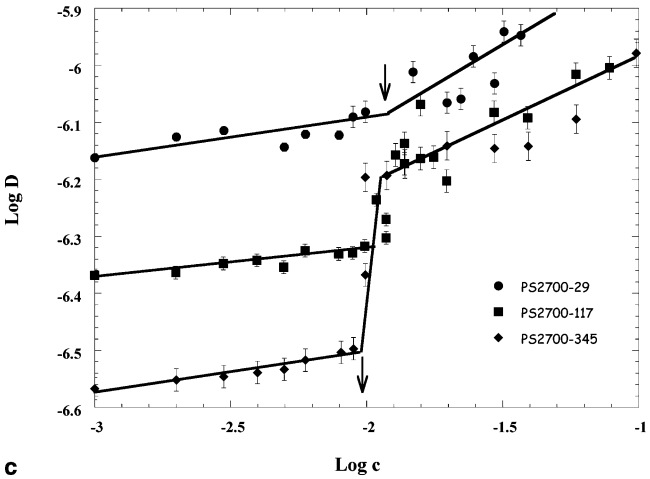

Figure 3. (a) Autocorrelation functions measured on the PS2700-345 system: at $c = 0.030$ g·mL^{-1} in THF, 25 °C for the angles shown. (b) Distribution of relaxation time on the PS2700-345 system: $c = 0.030$ g·mL^{-1} in THF, 25 °C at the scattering angle $\theta = 40°$. (c) Influence of the degree of polymerization of the main chain: PS branch molar mass = 2700 g mol^{-1} THF, 25 °C, log $D = f(\log c)$.

lective motion of the PM's branches. In other words, in a nondilute regime of concentration, the PMs diffuse in the medium, crowded by others, by multiple and collective relaxations of the branches (and not internal

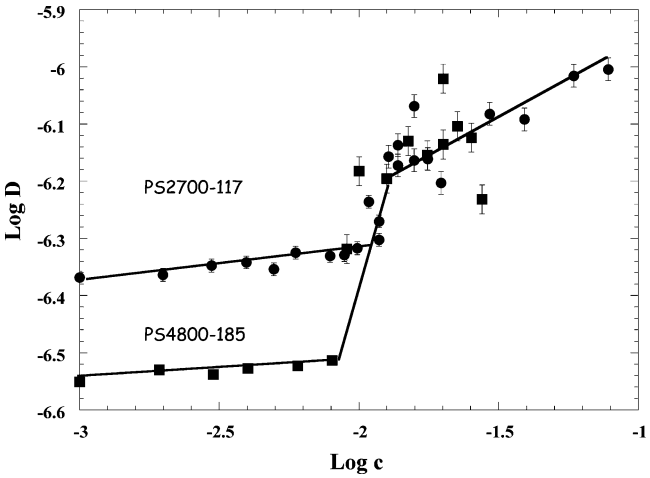

Figure 4. Influence of the degree of polymerization of the side chain: (●) PS branch molar mass = 2700 g mol^{-1}; (■) PS branch molar mass = 4800 g mol^{-1}. THF, 25 °C, log $D = f(\log c)$.

Table 2. Investigated Systems

sample	L_{MC}/L_{2bPS}[a]	sample	L_{MC}/L_{2bPS}[a]
PS2700-29	1.4	PS4800-25	0.7
PS2700-117	5.65	PS4800-185	5.1
PS2700-345	16.75	PS4800-290	7.95

[a] L_{MC} is the theoretical length of the main-chain in extension, and L_{bPS} is the theoretical length of the PS branches in extension.

dynamics) that ultimately lead to the diffusion of the overall PM. It is this collective motion of the branches that at the origin of the nondependency (or very little) of the diffusion coefficient vs the concentration.

It is interesting to note that such a transition in the diffusion coefficient variation as a function of c was not observed by Vlassopoulos et al.[16] Our system differs from Vlassopoulos et al.[16] 's work in that (i) the $DP_{n\ MC}$ (10 and 40) are much shorter than ours, and hence their PM are expected to behave much more like star polymers than ours, and (ii) the sizes of the backbone monomer unit differ. In our case, it is the ω-norbonenyl polystyrene that constitutes the monomer and is polymerized to give rise to PMs with polynorbornene backbone while Vlassopoulos et al. investigate PM with PMMA (or PS) backbone with PMMA (or PS) branches. Therefore, the distance between branches differs between the two kinds of PM.

Therefore, the transition-like change observed in the so-called collective dynamics[33−40] illustrated by D vs the concentration in the nondilute regime, besides the fact that it is related to the osmotic compressibility of the system, might have it origin strongly related to the difference in length in the backbone and the branches and the size of the monomer (and therefore to the local conformation of the PMs) and their interactions.[41−46]

III.3. Comparison of PS2700-29 with a Polynorbornene Linear Chain ($\overline{DP_n}$ = 370). DLS measurements have been also carried out in THF at 25 °C on a polynorbornene linear chain. Figure 5 shows the variation of the diffusion coefficient D vs c for PS2700-29 (M_w = 78 500 g mol^{-1}) and the polynorbornene sample (M_w = 35 000 g mol^{-1}). The deduced translational diffusion $D^0 = 5.88 \times 10^{-7}$ cm^2·s^{-1}, hydrodynamic radius $R_h{}^0{}_{PNB}$ = 8.1 nm and virial dynamic $k_D = 3.20$ are also reported in Table 3. One observes that even for polynorbornene of small molar mass (M_w = 35 000 g mol^{-1}) compared

Table 3. Dilute Solutions: DLS Measurements

sample	translational diffusion coeff D_0 (10^7cm^2/s)	k_D virial dynamic	R_h^0 (nm)[a]	L_{bPS} extension (nm)[b]
PS2700-29	7.1 ± 0.4	7.2 ± 0.4	6.7 ± 0.3	6.45 ± 0.3
PS2700-117	4.2 ± 0.2	12.5 ± 0.6	11.2 ± 0.6	6.45 ± 0.3
PS2700-345	2.6 ± 0.1	22 ± 1	18 ± 1	6.45 ± 0.3
PS4800-25	4.9 ± 0.2	12.1 ± 0.6	9.62 ± 0.5	11.63 ± 0.6
PS4800-185	2.8 ± 0.1	10.1 ± 0.5	17.0 ± 0.8	11.63 ± 0.6
PS4800-290	2.4 ± 0.1	13.2 ± 0.7	20 ± 1	11.63 ± 0.6
polynorbornene ($\overline{DP_n}$ = 370)	5.9 ± 0.3	3.2 ± 0.2	8.10 ± 0.4	

[a] Effective values deduced from the measured D_0 using Stokes−Einstein equation. [b] Length of the polystyrene branch assumed to be fully extended and calculated considering the vinylic monomer length equal to 2.52 Å.

Table 4. Calculations of Experimental Values Obtained in Dilute Solution

	prolate ellipsoid model (a, b = respectively major and minor axis)		Yamakawa−Fujii model		
sample	$d = 2b$[a] (nm)	L_{NB}[b] $= 2a - 2b$ (nm)	d (nm)	L (nm)	l_K (nm)
PS2700-117	13.6 ± 0.7[c]	29.0 ± 1.5	13.6 ± 0.7[c]	29.0 ± 1.5[c]	68.5 ± 3.4
PS2700-345	13.6 ± 0.7[c]	82.0 ± 4.1	13.6 ± 0.7[c]	94.5 ± 1.5	68.5 ± 3.4[c]
PS4800-185	20 ± 1[c]	50.3 ± 2.5	20 ± 1[c]	50.3 ± 2.5[c]	115 ± 6
PS4800-290	20 ± 1[c]	72.0 ± 3.6	20 ± 1[c]	82.0 ± 4.1	115 ± 6[c]

[a] b is assumed to be equal to the hydrodynamic radius of the spherical form: $b_{PS2700} = R_h{}^0_{PS2700-29}$ and $b_{PS4800} = R_h{}^0_{PS4800-25}$. [b] L_{NB} is the length of the PM and is deduced from the calculation. [c] Fixed value.

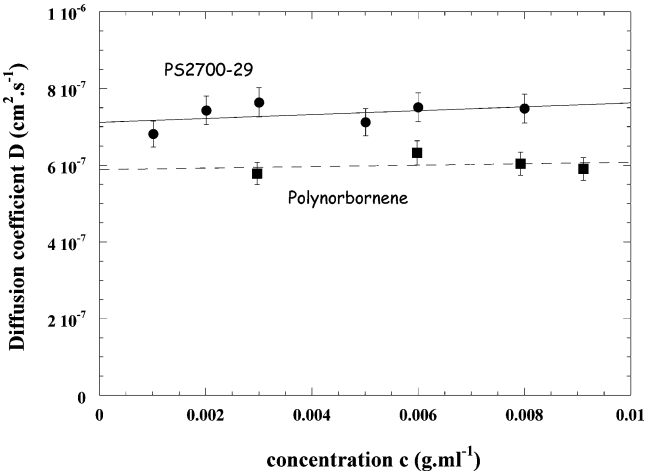

Figure 5. Comparison between a linear polynorbornene (DP_n = 370) and PM PS2700-29.

Table 5. Determination of $[\eta]$, R_v (nm), and R_v/R_h

	$[\eta]$ (mL/g)			
sample	Huggins	Kraemer	R_v (nm)	R_v/R_h
PS2700-29	16.5	16.2	5.5 ± 0.5	0.88 ± 3%
PS2700-117	17.5	17.7	9.6 ± 0.4	0.85 ± 3%
PS2700-345	15.35	16.1	13.3 ± 0.2	0.74 ± 5%

to that of the polymacromonomer PS2700-29 (M_w = 78 500 g mol^{-1}), the hydrodynamic radius $R_h{}^0_{PNB} = 8.1$ nm > $R_h{}^0_{PS2700-29} = 6.67$ nm. This is a direct evidence that PMs are compact objects compared to linear coils.

III.4. Viscosity Measurements. PS2700-based PM samples have been investigated by viscosity measurements. Intrinsic viscosities in dilute solutions, $[\eta]$, were obtained using both the Huggins (relation 9) and the Kraemer (relation 10) equations.

$$\eta_{sp}/c = [\eta] + k_H[\eta]^2c + ... \quad (9)$$

$$\ln \eta_r/c = [\eta] - k_K[\eta]^2c + ... \quad (10)$$

The intrinsic viscosities $[\eta]$ were then determined by linear regression and extrapolation to the very low concentration domain (see Figure 6, parts a and b, and Table 5). Both methods gave roughly the same result. Viscosimetric radii R_V have also been estimated from $[\eta]$ according to

$$R_V = \left[\frac{3}{10\pi N_A}\right]^{1/3}([\eta]M_{app})^{1/3} \quad (11)$$

Our results show that the ratio R_v/R_h decreases when the degree of polymerization of the PMs increases. This suggests also that the morphology is changing from a more or less spherical shape (PS2700-29; $R_v/R_h = 0.88$) to a nonspherical shape for PS2700-345 ($R_v/R_h = 0.74$). One recalls that for hard spheres, the ratio R_v/R_h is equal to unity.

At higher concentrations, the reduced viscosity (η_{sp}/c) vs concentration plot is represented in Figure 6c (PS2700-117 and -345). Above a certain concentration a change in the slope of η_{sp}/c vs c is observed. The characteristic concentrations are $c = 7 \times 10^{-3}$ g mol^{-1} and $c = 9 \times 10^{-3}$ g mol^{-1} respectively, which correspond almost ideally to those determined by DLS. In this respect, the observation of an abrupt change in solution properties as a function of the concentration is substantiated. Concerning the PS2700-29 sample, measurements were not reproducible, unlike the case of PS2700-117 and -345 measurements. Given the fact that the flow times for PS2700-29 solutions were close to that of the pure solvent, errors were too large. On the other hand, no change in the slope of η vs c was really expected since no discontinuity was noticed in DLS measurements. More generally, η_{sp}/c generally decreases with $\overline{DP_{n\ MC}}$.

The viscosity behavior of these PMs is quite different from that of flexible polymer coils. Figure 6d illustrates the variation of η/η_0 vs the concentration for PS2700-117, PS2700-345, and linear coiled polystyrene PS-233K for comparison (molar mass for PS-233K is 2.33×10^5). Adjusting the experimental data to relation 9 or more precisely to relation 12 shows a clear deviation for PMs systems and a good agreement for coil flexible PS ($[\eta]$ = 77 and $k_H = 0.43$). The obtained values of k_H for PMs are orders of magnitude higher compared to flexible coil PS in good solvent.

$$\eta/\eta_0 = 1 + [\eta]c + k_H[\eta]^2c + ... \quad (12)$$

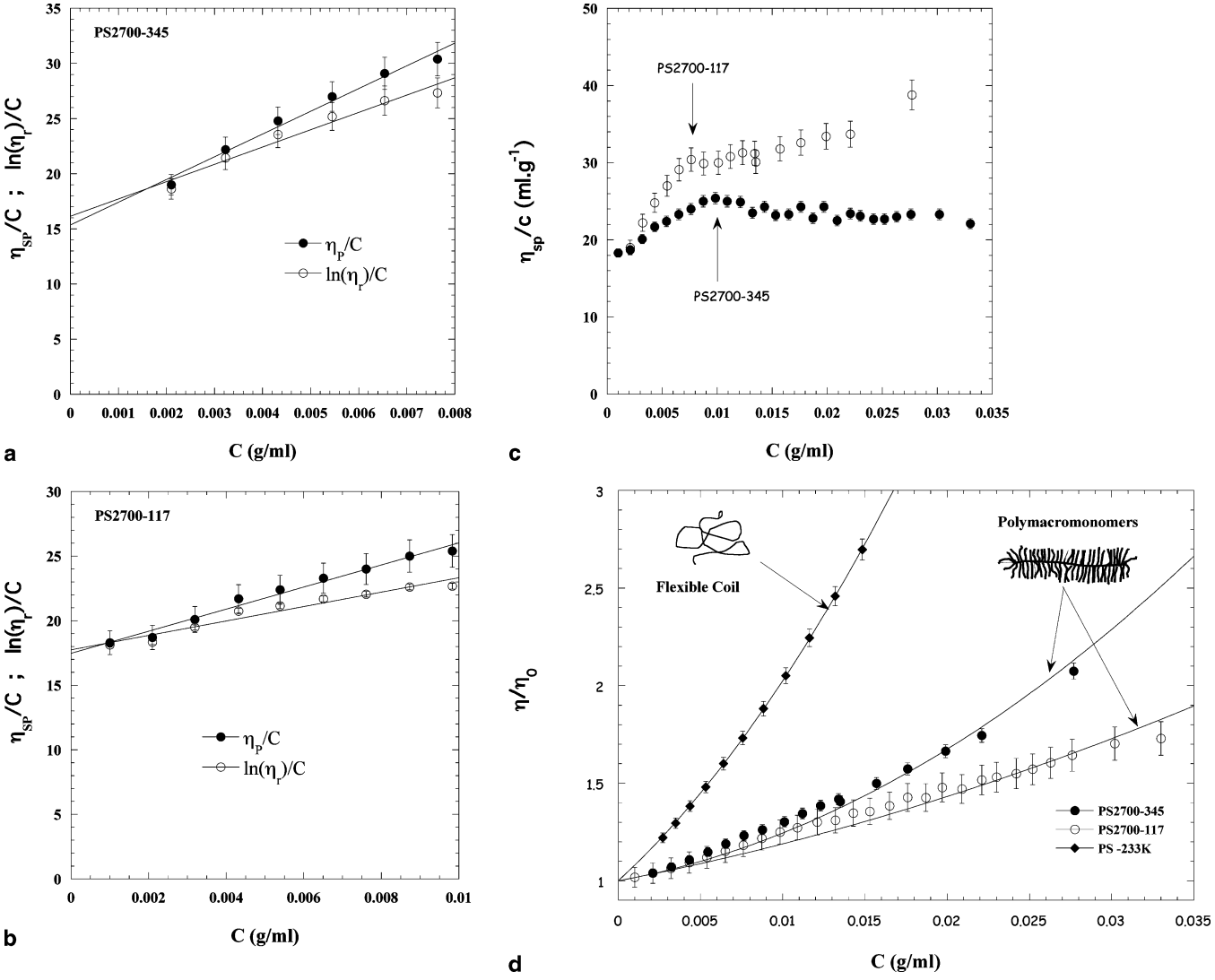

Figure 6. (a) Huggins and Kraemer representation of the intrinsic viscosity [η] PS2700-345 system. (b) Huggins and Kraemer representation of the intrinsic viscosity [η] PS2700-117 system. (c) Influence of the backbone length on viscosity behavior; branch molar mass M_w = 2700 g mol^{-1} PS2700-117 and -345, $\eta_{sp}/c = f(c)$. (d) Variation of η/η_0 vs the concentration for PS2700-117, PS2700-345, and PS-233K.

This noncoil viscosity behavior can also be highlighted when comparing the macro and the microviscosities.[32] Indeed, the ratio of the microviscosity η_μ ($\eta_\mu = k_BT/6\pi DR_h$, calculated from DLS results using the Stokes−Einstein relation) to the macroviscosity measured by a capillary viscometer shows also a very different behavior as a function of the concentration. For hard spheres, the ratio η_μ/η_{macro} is unity Stokes−Einstein behavior. For our PMs samples, it is not the case. These two quantities η_μ and η_{macro} and their ratio η_μ/η_{macro} are plotted as a function of c in Figure 7, parts a and b. One notes that for hard spheres, any deviation from this ratio should be compensated by the effective value of D or R_h at any concentration. This is obviously not the case as judge by the variation of η_μ and η_{macro} vs the concentration c. Indeed one observes a clear deviation from the Stokes−Einstein behavior. This deviation becomes less important for c lower than 1×10^{-2} g·mL^{-1} and is important for high $\overline{DP}_{n\ MC}$ as the concentration is increased.

III.5. Comparison with PS Stars. For star systems, the concentration dependence of Dc vs c above the overlap concentration c^* has been theoretically derived[47] taking into account of the core/shell contribution and leading to $D_c/D_0 \sim c^{0.77}[1 - 0.21\delta(c/c^*)^{-1.3}]$. Since PS2700-29 is assumed to adopt a spherical shape, only this sample is expected to exhibit a behavior comparable to that of the PS stars. Figures 8 and 9 show plots (log D vs log c) for each PS2700-based samples and its corresponding PS star. Obviously, PS2700-29 and PStetra20 exhibit similar behavior in the semidilute domain of PS2700-29, while a clear distinction can be observed between other PM systems and regular stars. Consequently, one can assert that the spherical shape of small $\overline{DP}_{n\ MC}$ PMs is firmly established through this comparison, whereas higher $\overline{DP}_{n\ MC}$ systems are shown to exhibit an elongated shape.

IV. Conclusion

In this study we have investigated the dynamical solution properties of PMs of different molar masses and branch lengths in good solvent. In dilute solutions and depending upon the backbone length and specific interactions, these PMs were found to adopt spherical, cylindrical, or wormlike morphologies and their dynamics is described by a single relaxation time. The variation of the single chain diffusion coefficient, $D_0 \propto M^{-1/3}$ reflects dense particle morphology. The results obtained,

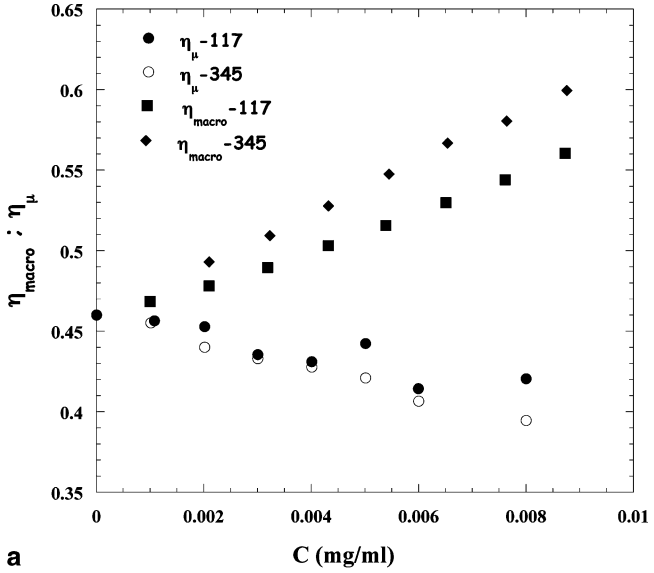

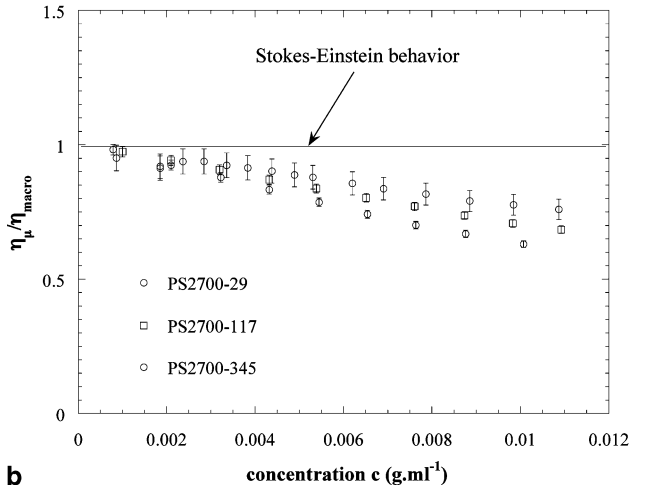

Figure 7. (a) Variation of η_μ and η_{macro} as a function of c for PS2700-117 and PS2700-345. (b) Variation of the ratio η_μ/η_{macro} as a function of c for PS2700-117 and PS2700-345.

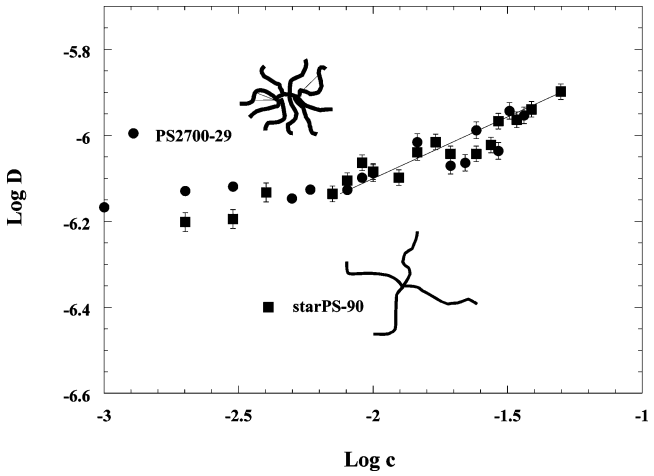

Figure 8. Comparison between PM PS2700-29 with starPS-90 (4 arms) (equivalent molar masses), THF, 25 °C. log D = f(log c).

using DLS and viscosity measurements suggest a dense and nonentangled particles as revealed by the low viscosity values and the scaling laws observed for the variation of the diffusion coefficient as a function of the molar mass and the concentration c. In nondilute

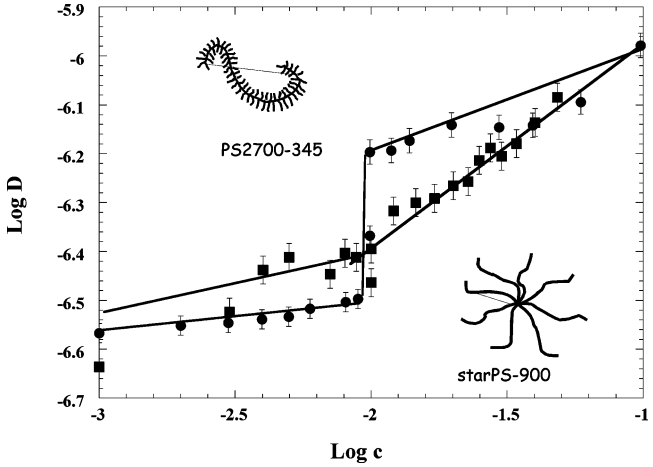

Figure 9. Comparison between PM (●) PS2700-345 with star (■) PS-900 (8 arms) (equivalent molar masses), THF, 25 °C. log D = f(log c).

regime, the dynamics is rather described by two relaxation times. The slow frequency is associated with the self-diffusion of the PM whereas the fast mode is identified as the collective diffusion coefficient. The transition from dilute to the nondilute regime is characterized by an abrupt increase of the diffusion coefficient with the concentration that coincides with the variation of the reduced viscosity η_{sp}/c vs c, as opposed to the case of linear and flexible polymer coils. Above this concentration, the diffusion coefficient is found to be independent of the molar mass and hardly varies with the concentration. It is identified as reflecting the overall collective motion of the branches (not an internal dynamics). This transition is also observed in the variation of the reduced viscosity η_{sp}/c as a function of c. Similar studies have been carried out on star polymers of roughly the same molar mass where no such an abrupt transition was observed.

Acknowledgment. The authors are grateful to Prof. Robert Pecora from the Chemistry Department, Stanford University, Palo Alto, CA, for helpful discussions.

References and Notes

(1) Burchard, W. *Adv. Polym. Sci.* **1999**, *143*, 113.
(2) Milkovich, R.; Chiang, M. T. US Patent 3,786,116, 1974.
(3) Ito, K.; Kawaguchi, S. PMs: Homo- and Copolymeriztion. *Adv. Polym. Sci.* **1999**, *142*, 128.
(4) Heroguez, V.; Gnanou, Y.; Fontanille, M. *Macromolecules* **1997**, *30*, 4791.
(5) Grande, D.; Six, J.-L.; Breunig, S.; Héroguez, V.; Fontanille, M.; Gnanou Y. *Polym. Adv. Technol.* **1998**, *9*, 601.
(6) Nemoto, N.; Nagai, M.; Koike, A.; Okada, S. *Macromolecules* **1995**, *28*, 3854.
(7) Wintermantel, W.; Gerle, M.; Fischer, K.; Schmidt, M.; Wataoka, I.; Urakawa, H.; Kajiwara, K.; Tsukahara, Y. *Macromolecules* **1996**, *29*, 978.
(8) Wataoka, I.; Urakawa, H.; Kajiwara, K.; Schmidt, M.; Wintemantel, M. *Polym. Int.* **1997**, *44*, 365.
(9) Terao, K.; Nakamura, Y.; Norisuye, T. *Macromolecules* **1999**, *32*, 711.
(10) Terao, K.; Hokajo, T.; Nakamura, Y.; Norisuye, T. *Macromolecules* **1999**, *32*, 3690.
(11) Terao, K.; Hayashi, S.; Nakamura, Y.; Norisuye, T. *Polym. Bull. (Berlin)* **2000**, *44*, 309.
(12) Fischer, K.; Schmidt, M. *Macromol. Rapid Commun.* **2001**, *22*, 787.
(13) Sheiko, S. S.; Gerle, M.; Fisher, K.; Schmidt, M. Möller, M. *Langmuir* **1997**, *13*, 5368.
(14) Gerle, M.; Fischer, K.; Roos, S.; Müller, M.; Schmidt, M.; Sheiko, S. S.; Prokhorova, S.; Möller, M. *Macromolecules* **1999**, *32*, 2629.

(15) Tsukahara, Y.; Miyata, M.; Senoo, K.; Yoshimoto, N.; Kaeriyama, K. *Polym. Adv. Technol.* **2000**, *11*, 210.
(16) Vlassopoulos, D.; Fytas, G.; Loppinet, B.; Isel, F.; Lutz, P.; Benoit, H. *Macromolecules* **2000**, *33*, 5960.
(17) Namba, S.; Tsukahara, Y.; Kaeriyama, K.; Okamoto, K.; Takahashi, M. *Polymer* **2000**, *41*, 5165.
(18) Tsukahara, Y.; Namba, S.; Iwasa, J.; Nakano, Y.; Kaeriyama, K.; Takahashi, M. *Macromolecules* **2001**, *24*, 2624.
(19) Birshtein, T. M.; Borisov, O. V.; Zhulina, Y. B.; Khokhlov, A. R.; Yurasova, T. A *Polym. Sci. USSR* **1987**, *29*, 1293.
(20) Zhang, M.; Breiner, T.; Mori, H.; Müller, A. H. E. *Polymer* **2003**, *44*, 1449.
(21) Zhang, M.; Drechsler, M.; Müller, A. H. E. *Chem. Mater.* **2004**, in press.
(22) Lesné, T.; Héroguez, V.; Gnanou, Y.; Duplessix, R. *Colloid. Polym. Sci. Short Commun.* **2001**, *279*, 190.
(23) Tsukahara, Y.; Kohjiya, S.; Tsusumi, K.; Okamoto, Y. *Macromolecules* **1994**, *27*, 1662.
(24) Tsukahara, Y. *Macromol. Rep.* **1995**, *32*, 821.
(25) Breunig, S.; Héroguez, V.; Gnanou, Y.; Fontanille, M. *Macromol. Symp.* **1995**, *95*, 151.
(26) Berne B. J.; Pecora, R. *Dynamic Light Scattering*; Wiley: New York, 1976.
(27) Siegert, A. J. F. Report No. 465, MIT rad. lab.; MIT: Cambridge, MA, 1943.
(28) Provencher, S. W. *Comput. Phys. Commun.* **1982**, *27*, 213. Provencher, S. W. *Comput. Phys. Commun.* **1982**, *27*, 229.
(29) Yamakawa, H.; Fujii, M. *Macromolecules* **1973**, *6*, 407.
(30) Duval, M.; Lutz, P.; Strazielle, C. *Makromol. Chem., Rapid Commun.* **1985**, *6* (2), 71.
(31) Lecommandoux, S.; Chécot, F.; Borsali, R.; Schappacher, M.; Deffieux, A.; Brûlet, A.; Cotton, J. P. *Macromolecules* **2002**, *35*, 8878.
(32) Tracy, M.; Jose Luis Garcia, A.; Pecora; R. *Macromolecules* **1993**, *26*, 1862.
(33) Doi, M.; Edwards, S. F. *The theory of polymer dynamics*; Clarendon Press: Oxford, England, 1986.
(34) Roovers, J. E. L.; Bywater. S. *Macromolecules* **1972**, *5*, 384.
(35) Huber, K. Burchard, W.; Fetters, L. J. *Macromolecules* **1984**, *17*, 541.
(36) Noda, I.; Horikawa, T.; Kato, T.; Fujimoto, T.; Nagasawa, M. *Macromolecules* **1970**, *3*, 795.
(37) Aberlea, T.; Burchard, W. *Comput. Theor. Polym. Sci.* **1997**, *3*, 215.
(38) Santosh, K.; Gupta, K.; Kumar, A.; Deo, S. R. *Polymer* **1978**, *19*, 895.
(39) Khokhlov, A. R.; Lomonosov, M. V. *State Univ., Moscow, USSR Polym. Sci. U.S.S.R.* **1978**, *20*, 2091.
(40) Schmidt, M.; Nerger, D.; Burchard, W. *Polymer* **1979**, *20*, 582.
(41) Roovers, J. E. L. *Polymer* **1975**, *16*, 827.
(42) Strazielle, Cl.; Herz, *J. Eur. Polym. J.* **1977**, *13*, 223.
(43) Burchard, W.; Schmidt, M.; Stockmayer, W. H. *Macromolecules* **1980**, *13*, 1265.
(44) Kato, T.; Miyaso, K.; Noda, I.; Fujimoto, T.; Nagasawa, M. *Macromolecules* **1970**, *3*, 777.
(45) Burchard, W. *Adv. Colloid Interface Sci.* **1996**, *64*, 45.
(46) Candau, F.; Strazielle, Cl.; Benoit, H. *Eur. Polym. J.* **1976**, *2*, 95.
(47) Semenov, A. N.; Vlassopoulos, D.; Fytas, G.; Vlaschos, G.; Fleischer, G.; Roovers, J. *Langmuir* **1999**, *15*, 358.

MA0487958